Journal of Solid State Chemistry **148,** 442–449 (1999)
Article ID jssc.1999.8477, available online at http://www.idealibrary.com on IDEAL®

$Sc_2B_{1.1}C_{3.2}$, a New Rare-Earth Boron Carbide with Graphite-like Layers

Ying Shi, A. Leithe-Jasper, L. Bourgeois, Y. Bando, and T. Tanaka[1]

National Institute for Research in Inorganic Materials, Namiki 1-1, Tsukuba, Ibaraki 305-0044, Japan

Received February 22, 1999; in revised form July 21, 1999; accepted August 10, 1999

A Sc-based boron carbide $Sc_2B_{1.1}C_{3.2}$ with a two-dimensional graphite-like framework has been synthesized by a solid state chemical reaction route. Crystals have been grown successfully and the crystal structure could be assigned to represent a new structure type of rare-earth boron carbides. The trigonal crystal structure ($a = b = 23.710(9)$ Å, $c = 6.703(2)$ Å, $P\bar{3}m1$ (No. 164)) is composed of alternate $-[B_{1/3}C_{2/3}]_\infty$–Sc–C–Sc–$[B_{1/3}C_{2/3}]_\infty-$ layers. The boron and carbon atoms $-[B_{1/3}C_{2/3}]_\infty-$ form a significantly puckered graphite-like layer in a rather disordered way. The Sc–C–Sc units appear to be rather loosely accommodated between the $[B_{1/3}C_{2/3}]_\infty$ units. Sc–Sc distances show a very close metal–metal contact. In the Sc–C–Sc units carbon atoms are surrounded by six Sc atoms in the form of a slightly distorted octahedron.

Key Words: **crystal structure; scandium boron carbides; $Sc_2B_{1.1}C_{3.2}$; graphite-related compound; EELS; HRTEM.**

1. INTRODUCTION

Ternary boron carbides of rare-earth and actinide metals have been the subject of continuous scientific interest with regard to a variety of structures and chemical and physical properties (1). From examining the phase diagram of the Sc–B–C system (2), a novel compound with nominal chemical formula Sc_2BC_3 was found. The X-ray powder diffraction (XRD) and electron diffraction pattern (EDP) of a Sc_2BC_3 powder indicated that this compound has a two-dimensional incommensurate structure, with a basic hexagonal unit cell of $a = b = 3.3991(2)$ Å, $c = 6.7140(6)$ Å. Crystals have been grown successfully and the crystal structure could be assigned to represent a new rare-earth boron carbide structure type with an unusual two-dimensional graphite-like $[BC]_\infty$ framework.

In the carbides studied so far the carbon units are restricted to isolated atoms or C_2 chains, or even C_3 units in Sc_3C_4 (3). In ternary compounds of boron and carbon with rare-earth or transition metals the nonmetal atoms generally form either two dimensional (2-D) networks, monodimensional (1-D) zigzag chains, or finite linear units of various length inserted in a metallic matrix (4, 5). Up to now only three compounds have been reported with the $[BC]_\infty$ graphite-like framework, LiBC (6), MgB_2C_2 (7), and BC_3 (8). The planar $[BC]_\infty$ layers of the first two compounds are isostructural to graphite layers and the stacking is like that of BN with a C–B–C–B sequence in adjacent layers. Although the information about the atomic structure of the BC_3 compound is limited and the BC distribution has not been unambiguously determined experimentally, this compound has been the subject of extensive research for carbon nanotube synthesis and related electronic structure investigations (9, 10). Thus the structure determination of new graphite-related compounds becomes more interesting owing to the fact that the compounds could combine desired materials with interesting physical properties.

2. EXPERIMENTAL PROCEDURES

2.1. Single Crystal Growth

Polycrystalline sintered rods of Sc_2BC_3 were used as feed and seed rods. They were prepared by solid state reaction as described in Ref. (2). The starting materials were Sc_2O_3 powder (4N, Crystal System Inc., Japan), amorphous boron (3N, SB-Boron Inc., USA), and graphite (3N, Koujundo Kagaku Co., Japan). First, scandium carbide Sc_2C_{1-x} was synthesized by using a carbo-thermal reduction method. Then the desired amount of carbon and boron were added to the scandium carbide powder. Stoichiometric mixtures of powders were isostatically pressed into rods at 250 MPa. The rod was reacted at about 1700°C in vacuum for at least 10 h in a boron nitride crucible which was inserted into an inductively heated graphite susceptor. Temperature was measured using an optical pyrometer (0.65 μm) by simulating black body condition through a small drilled hole in the crucible lid. In order to obtain equilibrium, all the rods were crushed, reshaped, and subjected to at least a second annealing.

The crystal was grown by a floating-zone method in a xenon-lamp image furnace under continuous flow of Ar (99.999 wt%) gas. Both the feed rod and the growing crystal

[1] To whom correspondence should be addressed. Fax: 81-298-51-6280. E-mail: Tanakat@nirim.go.jp.

0022-4596/99 $30.00

were synchronously driven downward at a rather low speed of 2 mm/h under counterrotation of 35 rpm. The details of the crystal growth will be published elsewhere.

2.2. Characterizations

After the powder was dissolved into an $HNO_3 + HCl$ (1 : 1) solution which was kept at 150°C for 16 h, the scandium and boron contents were determined by chelate titration and inductively coupled plasma atomic emission spectroscopy, respectively. The carbon content was determined by a volumetric combustion method using a carbon determinator (WR-12, Leco Co.). Oxygen impurity was analyzed by a standard inert gas fusion method (TC-136, Leco Co.).

The electron diffraction patterns were obtained at an acceleration voltage of 100 kV using a standard transmission electron microscope (Hitachi H-500). The high-resolution transmission electron microscopy (HRTEM) observations were carried out using a field-emission JEM3000F (JEOL) instrument operated at 300 kV, and equipped with a parallel electron energy loss spectrometer (EELS) (Gatan 666 model). Stationary electron probes focused down to 1 nm were used for collection of the EELS spectra. Computer simulations of high resolution images were obtained thanks to the Mac Tempas simulation package by taking into account the electron optical parameters of our HRTEM instrument. The presented simulations were all chosen very near the optimum defocus condition.

The X-ray reflections of a single crystal were collected on an Enraf–Nonius CAD4 automatic four-circle diffractometer with graphite monochromated Mo$K\alpha$ radiation. The intensity data were corrected for Lorentz and polarization effects. The absorption correction applied to the collected data was based on a Gaussian numerical integration employing the measured dimension of the single crystal (11).

3. RESULTS AND DISCUSSION

3.1. Determination of Structure

The chemical analysis of two pieces cut from different crystals show nearly the same composition of $Sc_2B_{1.11}C_{3.24}$ with an oxygen impurity content of about 0.80 wt%. Therefore $Sc_2B_{1.1}C_{3.2}$ is used to represent this new compound. The EDP shown in Fig. 1a for a $Sc_2B_{1.1}C_{3.2}$ single crystal in the a^*–b^* plane could be interpreted clearly by a two-dimensional commensurate 7×7 superlattice structure of the basic unit cell obtained from XRD and EDP analysis of the powder sample (the EDP of the powder sample is shown in Fig. 1b, where an incommensurate superlattice structure can be observed). The crystallization obviously causes a phase transition from an incommensurate to a commensurate structure.

Pieces cut from one grain were examined using a Weissenberg camera. A trigonal or hexagonal lattice showing no special extinctions was confirmed. The initial structure solution trial was based on a basic unit cell with $a = b =$ 3.3879(2) Å and $c = 6.7030(5)$ Å. The reflection intensities of the strong reflections satisfy the condition of $hkl = khl$, which suggests three possible space groups, $P\bar{3}m1$ (No. 164), $P3m1$ (No. 156), and $P321$ (No. 150). Because the X-ray scattering power of the boron and carbon atoms are very

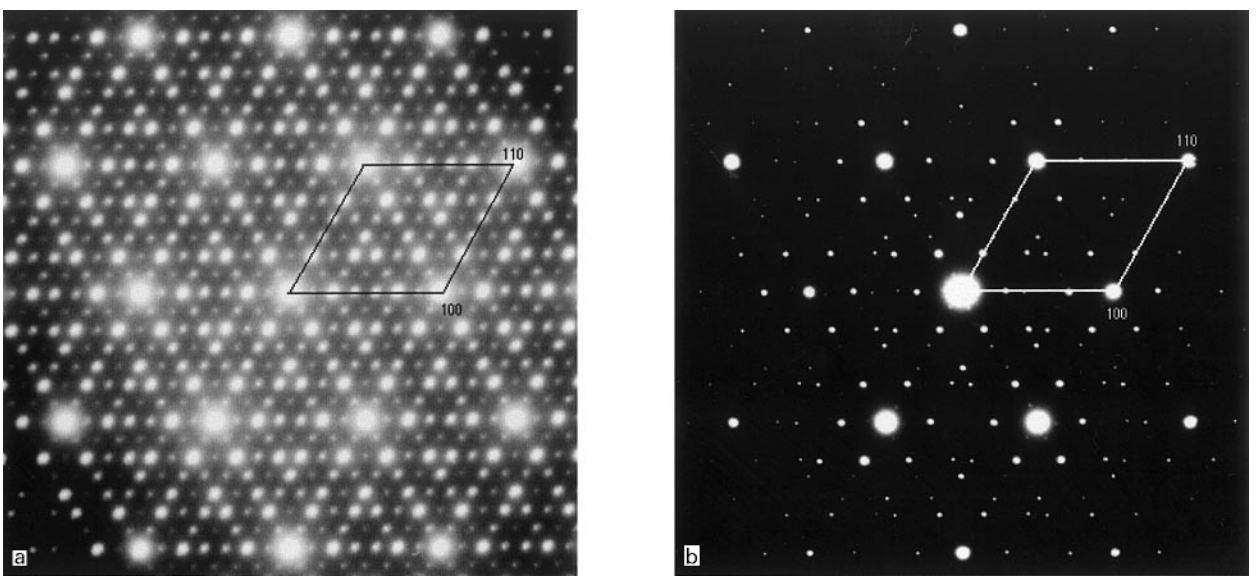

FIG. 1. Electron diffraction patterns of the $Sc_2B_{1.1}C_{3.2}$ compound from (a) a single crystal (commensurate structure) and (b) a powder sample (incommensurate structure), with the electron beam parallel to the [001] axis.

close, at the first stages of refinement all the nonmetal B or C positions were assigned to be C atoms. A structural model based on $-C_{z\approx 0}-Sc_{z\approx 1/3}-C_{z\approx 1/2}-Sc_{z\approx 2/3}-C_{z\approx 0}-$ (Z: Z-positional parameter) units could be derived for all the three possible space groups. Two Sc layers occupied the planes $Z = 1/3$ and 2/3, respectively, with very short bond lengths, even a little shorter than the value of 3.28 Å observed in h.c.p. Sc metal (12). The middle $C_{z\approx 1/2}$ layer was on the plane $Z = 1/2$ in the interstices of the Sc-layers. The $C_{z\approx 0}$ layer on the plane $Z = 0$ exhibited a two-dimensional network. Since the isotropic displacement parameters of the $C_{z\approx 0}$ atoms were up to seven times higher than those of Sc and $C_{z\approx 1/2}$ atoms, and several Fourier peaks with high intensities were found in this layer, it was therefore concluded that the incommensurate structure observed in the powder sample most likely was caused by disorder in the arrangement of the $C_{z\approx 0}$ atoms.

Thus the final structure solution was based on an unit cell ($a = b = 23.710(9)$ Å and $c = 6.703(2)$ Å) taking full account of the 7×7 superlattice and the basic structure arrangement found in the small unit cell. Details of the data collection are given in Table 1. Of the 1292 reflections with intensities $F_0 > 4\sigma(F_0)$ there are 1084 reflections required by a 7×7 superlattice. The highest symmetry space group $P\bar{3}m1$ (No. 164) was tried first and further structure refinement verified this choice. Based on the 12 individual Sc positions found by the SIR92 (13) ($R = 48.35$) direct methods program, the $C_{z\approx 1/2}$ positions were identified with a difference Fourier synthesis, and their location could be unambiguously correlated with the number and the height of the resulting eight Fourier peaks ($R = 16.1$). Their position inside a densely packed Sc layer was found to be similar to that in the structural model obtained with the small unit cell. A subsequent difference Fourier synthesis showed 18 peaks with close peak height and z-range and these peaks were therefore assigned to be $C_{z\approx 0}$ atoms. The refinement was carried out with the SHELX97 (14) program package.

TABLE 1
Crystal Data and Structure Refinement for $Sc_2B_{1.1}C_{3.2}$

Empirical formula	$C_{157}B_{54}Sc_{98}$
Formula weight	6881.00
Temperature	293(2) K
Wavelength	0.71073 Å
Crystal system, space group	Trigonal, $P\bar{3}m1$ (No. 164)
Unit cell dimensions	$a = b = 23.710(9)$ Å, $c = 6.703(2)$ Å
Volume	3263(2) Å^3
Z; calculated density	1; 3.501 Mg/m^3
Absorption coefficient	4.785 mm^{-1}
$F(000)$	3275
Crystal size	$0.2 \times 0.1 \times 0.06$ mm
Theta range for data collection	1.72° to 37.46°
Index ranges	$0 \le h \le 35$, $0 \le k \le 35$, $-7 \le l \le 11$
Reflections collected/unique	8284/6042 [R(int) = 0.0503, $R(\sigma)$ = 0.1403]
Completeness to 2theta = 74.91	99.9%
Refinement method	full-matrix least-squares on F^2 (SHELXL97)
Data/restraints/parameters	6042/0/168
Weighting scheme ($W = 1/[\sigma^2(F_o^2) + (0.0503 \times P)^2 + 0.00 \times P]$ where $P = [\mathrm{Max}(F_o^2) + 2 \times F_c^2]/3$	0.0490
Goodness of fit on F^2	1.096 [$F_o > 4\sigma(F_o)$]; 0.835 (all data)
Final R indices [$F_o > 4\sigma(F_o)$]	$R1 = 0.0461$, w$R2 = 0.1031$
R indices (all data)[a]	$R1 = 0.2575$, w$R2 = 0.1696$
Largest diff. peak and hole	1.526 and -1.300 e/Å^{-3}

[a] Because of the two-dimensional modulated structure in this large unit cell, only 1292 unique reflections have intensities with [$F_o > 4\sigma(F_o)$]. Therefore R indices for all reflection data are much higher than those for data with [$F_o > 4\sigma(F_o)$].

3.2. Atom Identification

If all the atomic positions are fully occupied according to the above model, there should be 98 Sc, 48 $C_{z\approx 1/2}$, and 162 $C_{z\approx 0}$ atoms in one unit cell. The boron and carbon distribution could not be assigned by comparison of the peak heights obtained from the difference Fourier synthesis. Although the peak heights for the $C_{z\approx 1/2}$ atoms are 4–5 times those of the $C_{z\approx 0}$ atoms, it is not sufficient to assign $C_{z\approx 1/2}$ as carbon because the peak heights of the electron densities are not only determined by the atomic numbers but are also very sensitive to bond length and coordination numbers of the atomic species. The peak heights in the $C_{z\approx 0}$ layer show some slight differences, but they are not obvious enough to distinguish between B and C atoms. Therefore the B and C distribution determination was thought to be based on the bond length comparison with those of known boron carbides.

In the $Sc_2B_{1.1}C_{3.2}$ structure the $C_{z\approx 1/2}$ atoms are accommodated in interstices of the dense Sc arrangement with a mean Sc–$C_{z\approx 1/2}$ distance of 2.294(17) Å. Every $C_{z\approx 1/2}$ atom is surrounded by six Sc atoms in the form of a slightly distorted octahedron. The long intralayer $C_{z\approx 1/2}$–$C_{z\approx 1/2}$ distance of 3.387(17) Å indicates that the $C_{z\approx 1/2}$ atoms are isolated. A similar interstitial accommodation can also be observed in numerous transition metal carbides (15). Similar bond lengths and coordination polyhedra of C-atoms can also be found in rare-earth carbides such as R_3C, R_2C (R refers to rare-earth) (16), and Sc_3C_4 (3). All of these bonding characteristics point to carbon and not boron, because B–Sc bond lengths are expected to be significantly larger. In ScB_2C_2 the average Sc–B bond distance is 2.51 Å (17) and for ScB_2C (18) a value of 2.543 Å can be calculated. In binary ScB_2 (19) (AlB_2 structure type) the Sc-B distance is 2.529 Å. The short distance between the Sc atoms of different layers in the [–Sc–$C_{z\approx 1/2}$–Sc] unit indicates that the C atom strengthens the metallic bond, which is in accordance with what can be seen in rare-earth carbides (16).

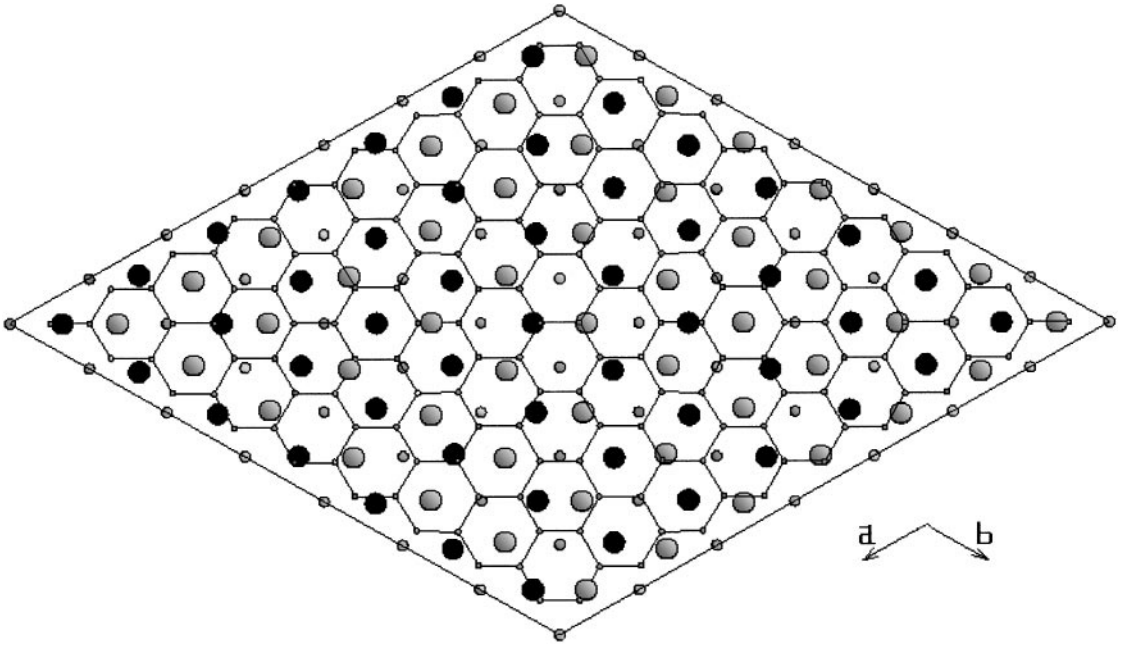

FIG. 2. Projection of the $Sc_2B_{1.1}C_{3.2}$ structure on the *a*–*b* plane. The carbon or boron atoms shown as small solid circles are connected to each other in a graphite-like layer within the range $z = -0.0855 \sim 0.0697$. The large open and filled circles represent scandium atoms in different layers. The $C_{z=1/2}$ carbon atoms are shown as medium filled circles.

If the $C_{z\approx 1/2}$ layer is now assigned to consist of carbon atoms, the $C_{z\approx 0}$ layer should be occupied by both boron and carbon atoms with the approximate atomic ratio 1 : 2 according to the chemical analysis result. EELS analysis strongly backs this assumption (see next section). A projection of the $Sc_2B_{1.1}C_{3.2}$ structure along [001] (Fig. 2) shows clearly that all the $C_{z\approx 0}$ atoms form a graphite-like layer. This layer is actually not flat but exhibits significant puckering. Positional *z*-parameters of the $C_{z\approx 0}$ show a distinct distribution around a mean $\bar{z} = 0.9896(13)$ value which gives rise to an "out of average plane" distance of 0.25(2) Å for the individual atoms. The projection on the (110) plane (Fig. 3) indicates a regular undulation in this layer. The $C_{z\approx 0}$–$C_{z\approx 0}$ in plane distances range from 1.478(18) to 1.577(11) Å with a mean value of 1.533(15) Å. This mean value is significantly larger than the graphite C–C bond length of 1.42 Å but shorter than the mean bond length 1.58 Å in the graphite-like compounds LiBC (6) and MgB_2C_2 (7) where B and C atoms could be distinguished. It is therefore almost impossible to determine the boron and carbon distribution in the graphite-like layer from bond length considerations. In addition to the very close and weak X-ray scattering power of B and C, an explanation for this ambiguous (B, C) distribution might be that B and C form a graphite-like layer in a disordered way but with some extent of preferred distribution on some special positions in the array. This is reflected by the bond length distribution in this layer. More than 80% of the bond lengths lie in the range of a ± 0.025 Å deviation from the mean value 1.533(15) Å. The rest includes short bonds of 1.478 Å (close to a graphite C–C bond length) and longer bonds of 1.577 Å (close to B–C bond length). From this bond length distribution the only definite conclusion that can be reached is that obviously no B–B bond exists in the

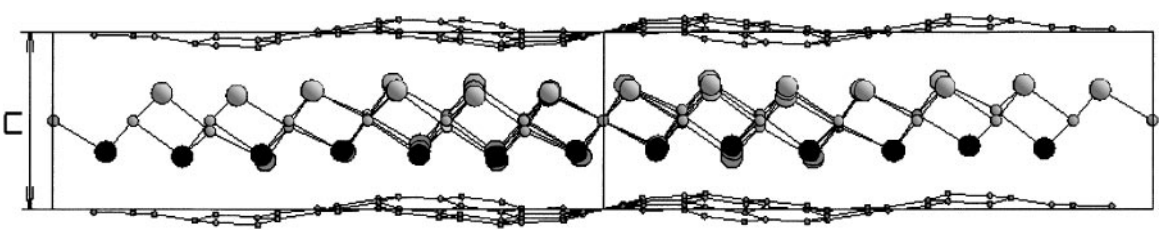

FIG. 3. Projection of the $Sc_2B_{1.1}C_{3.2}$ structure on the (110) plane. The atoms represented are the same as those in Fig. 2.

graphite-like layer, because the B–B bond length in six-membered rings is about 1.817 Å (19). If in the atom combinations with the longer bond lengths boron and carbon atoms were distinguished, the refinement of the whole crystal structure *R*-value could not be improved, and again one could not obtain a conclusive bonding scheme.

Refinement trials with regular arrangements of B and C in a 1 : 2 ratio on the basis of different geometrical combinations on a hexagonal graphite-like lattice layer were also by no means conclusive. Usually this kind of geometry implies a reduction of the whole space group symmetry from $P\bar{3}m1$ (No. 164) to $P3m1$ (No. 156). A transition to the space group with lower symmetry would lead to an increased number of parameters. Since already in the space group $P3m1$ (No. 164) the data/parameter ratio is low, it can not be expected that this transition leads to reliable results.

So the refinement trial was based on the assumption of a random distribution of B and C according to the ratio of 1 : 2 in the (B, C) layer. The final structure model $-[B_{1/3}C_{2/3}]_\infty-Sc-C-Sc-[B_{1/3}C_{2/3}]_\infty-$ with space group $P\bar{3}m1$ (No. 164) was therefore solved by the full-matrix least-square refinement. If scandium atoms were refined with anisotropic displacement parameters the final *R*-value was 4.61 for 1292 observations $[F_0 > 4\sigma(F_0)]$ and 168 variables. Refinement based on all the atoms with isotropic displacement parameters leads to an *R*-value 5.29 for 124 variables. The results with Sc refined by anisotropic displacement parameters are reported here. A final difference Fourier synthesis showed no maximum or minimum peaks above 1.53 $e/Å^3$. The results of the structure refinement including the atomic coordinates and equivalent isotropic displacement parameters are given in Table 2. Table 3 lists the anisotropic displacement parameters for the scandium atoms. The graphite-like layer seems to play a structure-governing role imposing a puckering also on the sandwiched –Sc–C–Sc– layer. As the data shows in Tables 2 and 3, both the atomic coordinates and the isotropic displacement parameters of B and C atoms have rather larger standard deviations than those of Sc atoms. It is believed that due to the low X-ray scattering power of B and C together with the low observable reflections ($F_0 > 4\sigma(F_0)$) and variables ratio (7.7) the positions of light atoms could not be determined very accurately. Selected bond distances are given in Table 4.

TABLE 2
Atomic Coordinates ($\times 10^4$) and Equivalent Isotropic Displacement Parameters ($Å^2 \times 10^3$) for $Sc_2B_{1.1}C_{3.2}$

Atom	Site	*X*	*Y*	*Z*	*U*(eq)[a]
Sc(1)	2d	3333	6667	3648(11)	5.4(3)
Sc(2)	12j	993(1)	7656(1)	6430(4)	6.2(4)
Sc(3)	12j	1946(2)	9599(1)	12992(3)	7.2(4)
Sc(4)	12j	433(2)	6650(1)	3088(4)	9.3(4)
Sc(5)	12j	1963(2)	6664(2)	3268(4)	8.5(6)
Sc(6)	12j	967(2)	6243(1)	6699(4)	8.4(5)
Sc(7)	6i	987(1)	9013(1)	16553(7)	6.1(5)
Sc(8)	6i	2349(1)	7651(1)	6695(7)	9.8(6)
Sc(9)	6i	494(3)	5247(2)	3305(4)	9.3(6)
Sc(10)	6i	479(2)	9521(2)	13248(6)	9.1(5)
Sc(11)	6i	2343(3)	6171(1)	7103(6)	12.4(8)
Sc(12)	6i	1930(1)	8070(1)	2781(4)	9.8(6)
C(13)	1b	0	10000	5000	8(3)
C(14)	6h	0	5717(6)	5000	8(3)
C(15)	6i	1431(4)	8569(4)	14414(13)	9(2)
C(16)	6i	1436(13)	5718(7)	5114(19)	8(3)
C(17)	6h	1442(9)	10000	15000	7(2)
C(18)	12j	1435(7)	7153(5)	4670(14)	9(2)
C(19)	6i	2857(5)	7143(5)	5330(2)	8(2)
C(20)	6h	0	7141(7)	5000	6(2)
BC(21)[b]	6i	1861(3)	8139(3)	−868(11)	6(2)
BC(22)	6i	2566(7)	6283(4)	701(17)	7(2)
BC(23)	12j	359(4)	6278(4)	−191(10)	6(1)
BC(24)	12j	1851(4)	9277(3)	9373(9)	4(1)
BC(25)	6i	1478(4)	8522(4)	9231(14)	11(2)
BC(26)	12j	1476(4)	9633(5)	9737(11)	6(1)
BC(27)	6i	1837(8)	5919(4)	10407(19)	12(2)
BC(28)	12j	1487(5)	7403(4)	9470(12)	11(1)
BC(29)	12j	729(4)	7014(4)	9550(10)	8(1)
BC(30)	6i	2950(4)	5900(8)	584(17)	9(2)
BC(31)	12j	367(4)	7402(5)	9719(10)	9(1)
BC(32)	12j	1480(5)	6289(5)	25(11)	8(1)
BC(33)	6i	728(3)	9272(3)	9776(15)	6(2)
BC(34)	6i	368(4)	9632(3)	9839(16)	7(2)
BC(35)	12j	1847(5)	7031(5)	−145(13)	11(1)
BC(36)	6i	2583(4)	7417(4)	196(19)	15(2)
BC(37)	12j	730(5)	5918(4)	60(10)	9(1)
BC(38)	6i	362(6)	5181(3)	9878(14)	10(2)

[a] *U*(eq) is defined as one-third of the trace of the orthogonalized U_{ij} tensor.

[b] BC represents the statistically distributed (B, C) atoms in the graphite-like $[-B_{1/3}-C_{2/3}-]_\infty$ layer.

TABLE 3
Anisotropic Displacement Parameters ($Å^2 \times 10^3$) for Sc Atoms of $Sc_2B_{1.1}C_{3.2}$

Atom	U_{11}	U_{22}	U_{33}	U_{23}	U_{13}	U_{12}
Sc(1)	5(2)	5(2)	6(2)	0	0	3(1)
Sc(2)	6(1)	5(1)	7(1)	−1(1)	1(1)	3(1)
Sc(3)	6(1)	6(1)	8(1)	−1(1)	0(1)	2(1)
Sc(4)	12(1)	7(1)	7(1)	−2(1)	0(1)	4(1)
Sc(5)	7(1)	6(1)	11(1)	−2(1)	0(1)	3(1)
Sc(6)	7(2)	11(1)	8(1)	0(1)	1(1)	6(1)
Sc(7)	7(1)	7(1)	4(1)	0(1)	0(1)	4(1)
Sc(8)	7(1)	7(1)	15(2)	0(1)	0(1)	4(1)
Sc(9)	12(2)	9(1)	8(1)	0(1)	0(1)	6(1)
Sc(10)	10(1)	10(1)	9(1)	−1(1)	1(1)	6(2)
Sc(11)	7(2)	16(2)	12(1)	1(1)	1(1)	4(1)
Sc(12)	8(1)	8(1)	7(1)	−1(1)	1(1)	0(1)

Note. The anisotropic displacement factor exponent takes the form $-2\pi^2[h^2a^{*2}U_{11} + \cdots + 2hka^*b^*U_{12}]$.

TABLE 4
Selected Bond Lengths (Å) for $Sc_2B_{1.1}C_{3.2}$

Sc(1)–C(19)	2.260(19)	Sc(2)–C(20)	2.253(3)	Sc(3)–C(20)	2.310(13)
Sc(1)–C(19)	2.260(19)	Sc(2)–C(18)	2.274(15)	Sc(3)–C(17)	2.297(16)
Sc(1)–C(19)	2.260(19)	Sc(2)–C(15)	2.310(9)	Sc(3)–C(15)	2.321(9)
Sc(1)–BC*(22)	2.527(14)	Sc(2)–BC(29)	2.476(7)	Sc(3)–BC(26)	2.469(8)
Sc(1)–BC(22)	2.527(14)	Sc(2)–BC(24)	2.533(7)	Sc(3)–BC(24)	2.518(6)
Sc(1)–BC(22)	2.527(14)	Sc(2)–BC(21)	2.545(7)	Sc(3)–BC(31)	2.662(8)
Sc(1)–BC(30)	2.587(14)	Sc(2)–BC(31)	2.556(7)	Sc(3)–BC(26)	2.677(9)
Sc(1)–BC(30)	2.587(14)	Sc(2)–BC(28)	2.566(9)	Sc(3)–Sc(2)	3.079(4)
Sc(1)–BC(30)	2.587(14)	Sc(2)–BC(25)	2.589(9)	Sc(3)–Sc(7)	3.106(4)
Sc(1)–Sc(11)	3.085(7)	Sc(2)–Sc(4)	3.050(4)	Sc(3)–Sc(3)	3.156(4)
Sc(1)–Sc(11)	3.085(7)	Sc(2)–Sc(3)	3.079(4)	Sc(3)–Sc(7)	3.273(3)
Sc(1)–Sc(11)	3.085(7)	Sc(2)–Sc(12)	3.114(4)	Sc(3)–Sc(2)	3.321(4)
Sc(4)–C(20)	2.293(13)	Sc(5)–C(18)	2.290(16)	Sc(6)–C(14)	2.292(4)
Sc(4)–C(14)	2.306(10)	Sc(5)–C(16)	2.306(15)	Sc(6)–C(16)	2.301(13)
Sc(4)–C(18)	2.315(14)	Sc(5)–C(19)	2.298(13)	Sc(6)–C(18)	2.311(11)
Sc(4)–BC(23)	2.341(7)	Sc(5)–BC(32)	2.410(8)	Sc(6)–BC(37)	2.356(7)
Sc(4)–BC(29)	2.501(7)	Sc(5)–BC(35)	2.511(9)	Sc(6)–BC(32)	2.514(8)
Sc(4)–BC(23)	2.655(9)	Sc(5)–BC(27)	2.522(10)	Sc(6)–BC(23)	2.560(8)
Sc(4)–Sc(6)	3.104(5)	Sc(5)–BC(36)	2.639(11)	Sc(6)–Sc(9)	3.059(4)
Sc(4)–Sc(4)	3.120(6)	Sc(5)–BC(22)	2.666(12)	Sc(6)–Sc(4)	3.299(6)
Sc(4)–Sc(6)	3.299(6)	Sc(5)–BC(30)	2.720(11)	Sc(6)–Sc(8)	3.307(3)
Sc(4)–Sc(3)	3.367(5)	Sc(5)–Sc(8)	3.075(4)	Sc(6)–Sc(4)	3.104(5)
Sc(4)–Sc(9)	3.409(4)	Sc(5)–Sc(6)	3.080(4)	Sc(6)–Sc(5)	3.080(4)
Sc(4)–Sc(2)	3.050(4)	Sc(5)–Sc(11)	3.130(5)	Sc(6)–Sc(2)	3.326(5)
Sc(7)–C(17)	2.279(3)	Sc(8)–C(19)	2.28(2)	Sc(9)–C(14)	2.279(10)
Sc(7)–C(17)	2.279(3)	Sc(8)–C(18)	2.317(13)	Sc(9)–C(14)	2.285(10)
Sc(7)–C(15)	2.322(16)	Sc(8)–C(18)	2.318(13)	Sc(9)–C(16)	2.284(26)
Sc(7)–BC(33)	2.408(11)	Sc(8)–BC(35)	2.514(10)	Sc(9)–BC(38)	2.313(10)
Sc(7)–BC(26)	2.520(8)	Sc(8)–BC(35)	2.513(10)	Sc(9)–BC(37)	2.587(7)
Sc(7)–BC(26)	2.520(8)	Sc(8)–BC(36)	2.536(14)	Sc(9)–BC(37)	2.584(8)
Sc(7)–BC(24)	2.623(8)	Sc(8)–BC(21)	2.584(12)	Sc(9)–BC(38)	2.764(11)
Sc(7)–BC(24)	2.623(8)	Sc(8)–BC(28)	2.601(11)	Sc(9)–Sc(9)	3.045(10)
Sc(7)–BC(25)	2.699(13)	Sc(8)–BC(28)	2.602(11)	Sc(9)–Sc(6)	3.055(4)
Sc(7)–Sc(10)	3.043(7)	Sc(8)–Sc(5)	3.074(4)	Sc(9)–Sc(4)	3.401(4)
Sc(7)–Sc(3)	3.106(4)	Sc(8)–Sc(12)	3.137(6)	Sc(9)–Sc(6)	3.059(4)
Sc(7)–Sc(3)	3.272(2)	Sc(8)–Sc(5)	3.075(4)	Sc(9)–Sc(4)	3.409(4)
Sc(10)–C(13)	2.289(6)	Sc(11)–C(16)	2.289(25)	Sc(12)–C(18)	2.271(10)
Sc(10)–C(17)	2.300(17)	Sc(11)–C(19)	2.326(12)	Sc(12)–C(18)	2.271(10)
Sc(10)–C(17)	2.303(17)	Sc(11)–C(19)	2.323(12)	Sc(12)–C(15)	2.322(17)
Sc(10)–BC(34)	2.329(12)	Sc(11)–BC(27)	2.446(14)	Sc(12)–BC(21)	2.462(8)
Sc(10)–BC(33)	2.542(11)	Sc(11)–BC(22)	2.455(12)	Sc(12)–BC(28)	2.621(9)
Sc(10)–BC(34)	2.731(10)	Sc(11)–BC(27)	2.444(14)	Sc(12)–BC(28)	2.620(9)
Sc(10)–BC(34)	2.729(10)	Sc(11)–BC(22)	2.453(12)	Sc(12)–Sc(2)	3.115(4)
Sc(10)–Sc(10)	3.063(7)	Sc(11)–Sc(5)	3.136(5)	Sc(12)–Sc(5)	3.396(7)
Sc(10)–Sc(10)	3.063(7)	Sc(11)–Sc(5)	3.135(5)	Sc(12)–Sc(4)	3.468(3)
Sc(10)–Sc(7)	3.043(7)	Sc(11)–Sc(6)	3.361(6)	Sc(12)–Sc(2)	3.114(4)
Sc(10)–Sc(10)	3.403(10)	Sc(11)–Sc(6)	3.359(6)	Sc(12)–Sc(5)	3.130(5)
Sc(10)–Sc(10)	3.403(10)	Sc(11)–Sc(1)	3.082(7)	Sc(12)–Sc(8)	3.137(6)
BC(21)–BC(28)	1.526(11)	BC(22)–BC(27)	1.509(22)	BC(23)–BC(23)	1.498(18)
BC(21)–BC(28)	1.526(11)	BC(22)–BC(30)	1.577(11)	BC(23)–BC(37)	1.511(12)
BC(21)–BC(25)	1.577(18)	BC(22)–BC(30)	1.577(11)	BC(23)–BC(29)	1.518(10)
BC(24)–BC(26)	1.519(13)	BC(25)–BC(24)	1.554(10)	BC(26)–BC(33)	1.537(11)
BC(24)–BC(25)	1.553(11)	BC(25)–BC(21)	1.577(18)	BC(26)–BC(26)	1.550(18)
BC(24)–BC(31)	1.554(10)	BC(25)–BC(24)	1.554(10)	BC(26)–BC(24)	1.519(13)
BC(27)–BC(32)	1.516(12)	BC(28)–BC(35)	1.527(14)	BC(29)–BC(23)	1.520(10)
BC(27)–BC(32)	1.517(12)	BC(28)–BC(21)	1.526(10)	BC(29)–BC(31)	1.544(12)
BC(27)–BC(22)	1.509(22)	BC(28)–BC(29)	1.557(14)	BC(29)–BC(28)	1.557(14)

TABLE 4—*Continued*

BC(30)–BC(36)	1.531(21)	BC(31)–BC(31)	1.553(15)	BC(32)–BC(27)	1.516(12)
BC(30)–BC(22)	1.577(11)	BC(31)–BC(24)	1.553(11)	BC(32)–BC(37)	1.539(12)
BC(30)–BC(22)	1.577(11)	BC(31)–BC(29)	1.544(12)	BC(32)–BC(35)	1.528(13)
BC(33)–BC(34)	1.478(18)	BC(34)–BC(33)	1.478(18)	BC(35)–BC(28)	1.527(14)
BC(33)–BC(26)	1.537(11)	BC(34)–BC(34)	1.526(15)	BC(35)–BC(36)	1.529(10)
BC(33)–BC(26)	1.537(11)	BC(34)–BC(34)	1.526(15)	BC(35)–BC(32)	1.528(13)
BC(36)–BC(35)	1.529(10)	BC(37)–BC(23)	1.511(12)	BC(38)–BC(38)	1.494(24)
BC(36)–BC(30)	1.531(21)	BC(37)–BC(38)	1.519(10)	BC(38)–BC(37)	1.518(10)
BC(36)–BC(35)	1.529(10)	BC(37)–BC(32)	1.539(12)	BC(38)–BC(37)	1.519(10)

[a] BC represents the statistically distributed (B, C) atoms in the graphite-like $[-B_{1/3}-C_{2/3}-]_\infty$ layer.

This model suggests the existence of some solid solution between boron and carbon in the graphite-like layer. At least 5% more boron substitution of carbon still gives the pure phase. Further investigation of the homogeneity range of this phase is now underway.

3.3. *EELS and HRTEM Results for $Sc_2B_{1.1}C_{3.2}$*

High-resolution transmission electron microscopy (HRTEM) and electron energy loss spectroscopy (EELS) were performed on small flakes of single crystalline $Sc_2B_{1.1}C_{3.2}$. The TEM sample was prepared by breaking a piece of $Sc_2B_{1.1}C_{3.2}$, scratching small specks from the bulk (thus using the material least exposed to air), grinding them in an agate mortar, and sonicating the resultant powder in CCl_4. The powder was then mounted onto a carbon-coated copper grid by floating the latter in the suspension.

Figure 4 shows the core-loss region of a typical EELS spectrum obtained from a $Sc_2B_{1.1}C_{3.2}$ crystallite. Three distinct features are apparent, at energies near 190, 290, and

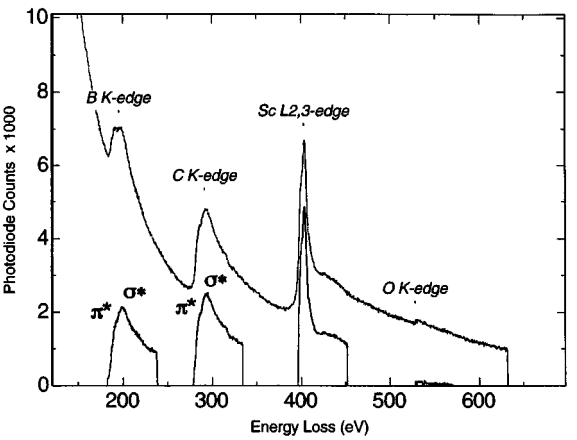

FIG. 4. Electron energy loss spectrum (EELS) of a $Sc_2B_{1.1}C_{3.2}$ crystal; also shown are the individual edges after background subtraction used for the atomic ratio calculation.

400 eV. They were identified as the boron and carbon K-edges and the $L_{2,3}$-edge of scandium, respectively. From the ionization cross sections calculated for each peak, atomic ratios between B, C, and Sc could be estimated. Atomic ratios of Sc/C = 0.68 and B/C = 0.32 were obtained, with uncertainty margins of about 10%. This is consistent with the chemical analysis result. A more detailed look at the K-edges of boron and carbon reveals the presence of two peaks for each edge. The small peak present at 188 eV for B and 285 eV for C corresponds to excitation of electrons into the π^* unoccupied electronic states. The main peak of each K-edge (at 200 eV for B and 291 eV for C) can itself be ascribed to the σ^* unoccupied states. While the σ^* peak reflects the presence of covalent bonds involving B and/or C, the σ^* peak is characteristic of a more or less planar trigonal network, similar to graphite. It can be deduced that B–C sp^2 (i.e., trigonal) bonds must be present. This strongly supports the idea of (B, C) layers. It is worth pointing out the similarity between these results and those obtained for the compounds BeB_2C_2 which also possess B–C sheets (20). The weakness of the π^* peak for both B and C may be explained by the puckered morphology of the (B, C) layers. The very weak oxygen K-edge could also be observed, which is consistent with the chemical analysis result of an oxygen impurity.

In Fig. 5 HRTEM lattice images are presented for the incident electron beam (a) roughly parallel to the basal planes and (b) perpendicular to the basal planes. Figure 5a clearly reveals the layer structure of the compound. Fringes can be seen to occur in bundles of three, each bundle being separated by 6.7 $\pm$ 0.1 Å. This distance is consistent with the lattice constant $c = 6.7$ Å obtained from X-ray diffraction. The three (dark) fringes making up each bundle are tentatively identified as the double Sc layer and the B–C graphitic layer of the structure model proposed on the basis of X-ray diffraction and EELS measurements. Since two of the three fringes seem slightly thicker than the third, they are assigned as Sc layers. This is illustrated schematically in the inset of Fig. 5a. A computer image simulation of the proposed structure is inset in the figure. The layer structure of the

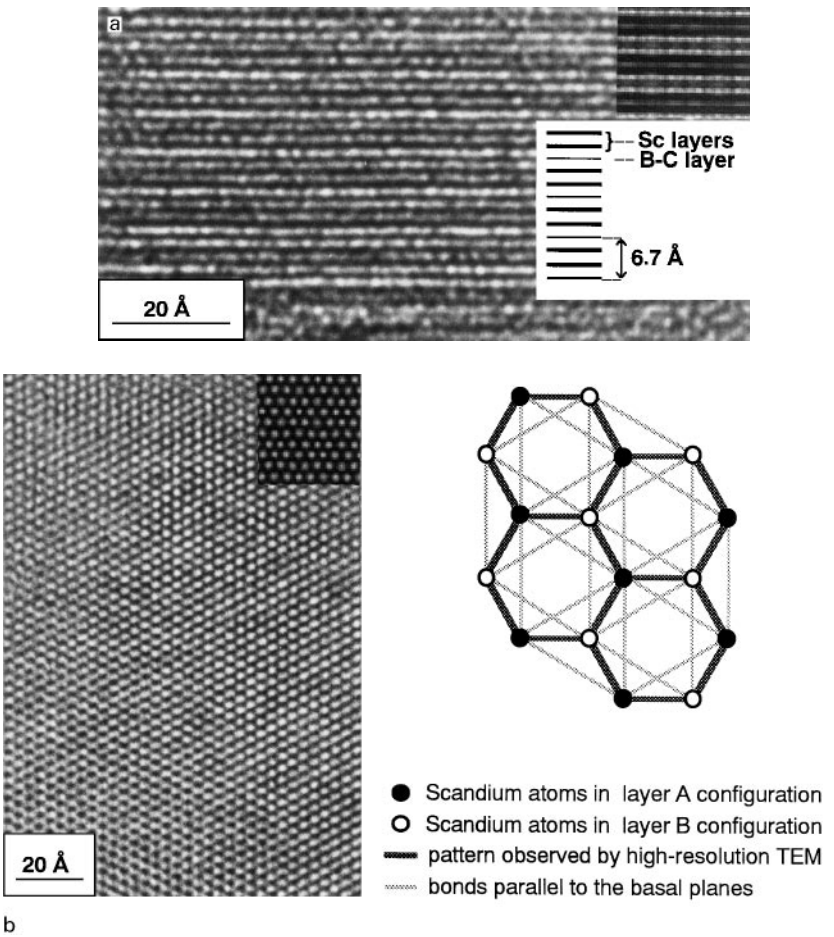

FIG. 5. High-resolution transmission electron microscopy (HRTEM) of an $Sc_2B_{1.1}C_{3.2}$ crystal with the incident electron beam (a) roughly parallel to the basal planes and (b) perpendicular to the basal planes. In each case computer simulated images of the proposed structure are inset.

compound is clearly revealed in the simulation. In Fig. 5b the basal planes of the crystal are imaged, showing clear white dots arranged in a hexagonal array. The distance between nearest neighbors of white dots was measured to be 3.3 ± 0.1 Å. This hexagonal pattern can be explained by considering that the Sc layers are stacked two by two according to the trigonal, i.e., ABAB …, configuration, as depicted in the inset. Therefore a high-resolution image of the Sc layers will show hexagons of Sc atoms with a black outline surrounding a white area. The distance between nearest white dot neighbors will then be the (100) distance of hexagonal Sc, or 3.3 Å, as observed. A computer simulated image (inset) confirms this.

It is not surprising that the information conveyed by the high-resolution images are dominated by Sc, as Sc is a much heavier atom than either B or C. In addition, there is evidence for considerable disorder in the B–C graphitic lattice from X-ray and electron diffraction. Such disorder is probably responsible for the absence of lattice information on the B–C layers shown in Fig. 5b. However, a preliminary study is suggesting that the periodic undulation of the (B, C) layer can sometimes be imaged. More detailed HRTEM and EELS work is now underway, in particular with the aim of ascertaining the bonding states of B and C atoms.

4. CONCLUSION

The crystal structure of $Sc_2B_{1.1}C_{3.2}$ is composed of alternate $-[B_{1/3}C_{2/3}]_\infty$–Sc–C–Sc–$[B_{1/3}C_{2/3}]_\infty-$ laminar layers. Boron and carbon atoms form a significantly puckered graphite-like layer with a mean bond length of 1.533(15) Å The "Sc–C–Sc" units appear to be rather loosely accommodated between the graphite-like $-[B_{1/3}C_{2/3}]_\infty-$ layers. This is reflected by the rather large mean Sc–$[B_{1/3}C_{2/3}]_\infty$ distance of 2.543(9) Å, whereas the mean Sc–Sc distance inside the Sc–C–Sc unit of 3.161(5) Å reflects a close metal–metal contact. In the Sc–C–Sc unit, six Sc atoms in the form of a slightly distorted octahedron surround the $C_{z=0.5}$ atoms. The coordination figures of the 12 Sc atomic positions can be roughly divided into three groups and are found to be composed of twelve atoms. Three carbons from Sc–C–Sc units are found in all of them. Sc and (B, C) atoms of the graphite-like layer in the Sc/(B, C) ratios of 3/6, 5/4, and 6/3 occupy the nine remaining positions. The rather complex arrangements reflect the modulated crystal structure.

Work improving the crystal quality is underway for physical property investigations.

ACKNOWLEDGMENTS

Ying Shi acknowledges JST for the support of an STA fellowship. The authors thank Mr. A. Sato for carrying out the four-circle data collection and Dr. X.A. Chen for useful discussion. They are also indebted to Dr. M. Uchida, Mr. S. Takenouchi, and Mr. Y. Yajima for electron diffraction and chemical analysis.

REFERENCES

1. P. Rogl, *in* "Phase Diagrams of the Ternary Metal–Boron–Carbon Systems" (G. Effenberg, Ed.). ASM International, Materials Park, OH, 1998.
2. Ying Shi, A. Leithe-Jasper, and T. Tanaka, submitted.
3. R. Pöttgen and W. Jeitschko, *Inorg. Chem.* **30,** 427 (1991).
4. J. Bauer, G. Boucekkine, G. Frapper, J.-F. Halet, J.-Y Saillard, and B. Zouchoune, *J. Solid State Chem.* **133,** 190 (1997).
5. D. Ansel, J. Bauer, F. Bonhomme, G. Boucekkine, G. Frapper, P. Gougeon, J.-F. Halet, J.-Y Saillard, and B. Zouchoune, *Angew. Chem. Int. Ed. Engl.* **35,** 2098 (1996).
6. M. Wörle, R. Nesper, G. Mair, M. Schwarz, and H. G. v. Schnering, *Z. Anorg. Allg. Chem.* **621,** 1153 (1995).
7. M. Wörle and R. Nesper, *J. Alloys Comp.* **216,** 75 (1994).
8. J. Kouvetakis, R. B. Kaner, M. L. Sattler, and N. Bartlett, *J. Chem. Soc. Chem. Commun.*, 1758 (1986).
9. Z. Weng-Sieh, K. Cherrey, N. G. Chopra, X. Blasé, Y. Miyamoto, A. Rubio, M. L. Cohen, S. G. Louie, A. Zettl, and R. Gronsky, *Phys. Rev. B* **51,** 11229 (1995).
10. D. Tománek, R. M. Wentzcovitch, S. G. Louie, and M. L. Cohen, *Phys. Rev. B* **37,** 3134 (1988).
11. B. A. Frenz and Associates, SDP for Windows Reference Manual, College Station, TX, 1995.
12. F. H. Spedding, A. H. Daane, and K. W. Herrmann, *Acta Crystallogr.* **9,** 559 (1956).
13. Altomare, G. Cascarano, C. Giacovazzo, A. Guagliardi, M. C. Burla, G. Polidori, and M. Camalli, *J. Appl. Crystallogr.* **27,** 435 (1994).
14. Sheldrick, G. M., Siemens Industrial Automation Inc., Madison, WI, 1994.
15. E. Parthe and K. Yvon, *Acta Crystallogr. B* **26,** 153 (1970).
16. G. Y. Adachi, N. Imanaka, and F. Z. Zhang, *in* "Handbook on the Physics and Chemistry of Rare-Earth" (K. A. Gschneidner and L. Eyring, Eds.), Vol. 15, p. 115, North Holland, Amsterdam, 1991.
17. G. S. Smith, Q. Johnson, and P. C. Nordine, *Acta Crystallogr.* **19,** 668 (1965).
18. J. Bauer, *J. Less-Common Met.* **87,** 45 (1982).
19. P. Peshev, J. Etourneau, and R. Naslain, *Mater. Res. Bull.* **5**, 319 (1970).
20. L. A. Garvie, P. R. Buseck, and P. Rez, *J. Solid State Chem.* **133,** 347 (1997).